Proceedings of the 9th World Congress on Momentum, Heat and Mass Transfer (MHMT'24)
London, United kingdom – April 11 – 13, 2024
Paper No. ENFHT 266
DOI: 10.11159/enfht24.266

Comparison Of The ORC And The PEORC For Low-Temperature Industrial Waste Heat Exploitation

Anastasios Skiadopoulos[1], Dimitrios Manolakos[1]
[1] Agricultural University of Athens, Department of Natural Resources Utilization and Agricultural Engineering
Iera Odos 75, Athens, Greece
tskiado@aua.gr; dman@aua.gr

Abstract **-** In this paper, the Organic Rankine Cycle (ORC) and the Partially Evaporated Organic Rankine Cycle (PEORC) were compared for low-temperature waste heat recovery, with a particular focus on industrial applications. Numerical models of the two power cycles were developed, while a dedicated two-phase expansion model simulating the performance of an industrial expander in the two-phase region was applied to estimate accurately the efficiency of the PEORC. Different WFs, temperatures of the heat source, and waste heat transfer rates were considered for a complete mapping of the power cycles' efficiency. The simulations indicate that the PEORC efficiency is highly dependent on the performance of the two-phase expander, with vapor quality at the evaporator outlet identified as the most crucial operating parameter. The comparison between the two power cycle architectures reveals that the PEORC performs consistently better, achieving thermal efficiencies between 2.28% and 7.75%, whereas, for identical operating conditions, the respective values for the ORC are in the range of 1.25% to 7.13%.

Keywords**:** Industrial waste heat; ORC; PEORC; Two-phase expansion modeling

1. Introduction

The optimal exploitation of energy sources is a prerequisite in the global effort to increase the sustainability of modern societies. One of the pillars on which this effort must be based is the improvement of the primary energy conversion efficiency of major energy consumers, such as in the industrial sector. Particularly in the industry, energy efficiency can be substantially increased by utilizing the large amounts of the generated waste heat from processes. Industrial waste heat is estimated to approach, on a global scale, nearly 70% of the primary energy input [1], with the highest share (rising to over 60% [1,2]) rejected at heat source temperatures lower than 100°C, a range commonly designated as low-temperature heat.

A common technological solution for the exploitation of low-temperature waste heat, directly applicable in the industry, is the installation of a bottoming power cycle. A well-established power cycle in the low-temperature heat range is the Organic Rankine Cycle (ORC), which can be driven by different heat sources, including waste heat, solar irradiance, geothermal power, and biomass. The ORC operates on the same principle as the steam Rankine Cycle, but the Working Fluid (WF) is selected among a variety of substances, such as refrigerants and hydrocarbons, with low boiling temperatures at high pressures. This flexibility in WF selection constitutes the main advantage of the ORC because the design of the power cycle can be adapted to the characteristics of the heat source. Furthermore, the type of power generator can be selected to maximize the efficiency of the ORC, with turbines typically applied in large-scale systems, and volumetric expanders, such as piston, twin-screw, scroll, and rotary vane, used in small-scale units [3]. The flexible design of the ORC has led to its wide-scale application, and it is now considered a mature and robust technology with low operating and maintenance costs, and nearly unsupervised operation [4].

The main drawback of the ORC is the increased exergy losses of the heat source during the evaporation of the WF [5]. The exploitation of the heat source's exergy can be increased by omitting the evaporation of the WF, in which case the power cycle assumes a trilateral shape, and an optimal match between the temperature profiles of the heat source and the WF is accomplished. The trilateral cycle is known as the Trilateral Flash Cycle (TFC), and it was originally conceived for the maximization of power generation in geothermal power plants [6,7]. The TFC consists of the same WF thermodynamic processes as the ORC, but the WF flows out of the evaporator in the saturated liquid state, and, thereafter, it undergoes two-phase expansion in the power generator. The TFC is realized by increasing the mass flow rate of the WF, leading to the absorption of higher amounts of heat from the WF, and, as a result, maximization of the generated power. The risk of erosion

by liquid droplets renders turbines unsuitable for two-phase expansion [8]. On the other hand, twin-screw expanders are indicated in the literature as the ideal expansion machine for the TFC [9] because of their ability to handle two-phase flows and operate at high rotational speeds with minimum friction losses. However, the very high volume ratios of the WF in the TFC cannot be easily handled by state-of-the-art twin-screw expanders applied in ORC units, with very low isentropic efficiencies documented in the literature when the expansion of the WF starts from the saturated liquid state [10,11]. To overcome this shortcoming of the TFC, the Partially Evaporating ORC (PEORC) power cycle was introduced, where a fraction of the WF's mass is evaporated, resulting in intermediate volume ratios during two-phase expansion. The PEORC combines the advantages of the ORC and the TFC, featuring increased heat source utilization compared to the ORC, and higher two-phase expansion efficiency than the TFC.

In this study, the PEORC and the ORC are compared for low-temperature waste heat recovery applications, relevant to the industry, with the maximum temperature of the heat source and heat duty reaching 100°C and 300 kW_{th}, respectively. For this purpose, a numerical model simulating the operation of the two power cycles under different temperatures of the heat source, heat duties at the evaporator, and different WFs was developed. The novelty of the presented herein work lies in the utilization of a novel semi-empirical thermodynamic model for the simulation of two-phase expansion in a twin-screw expander [12], instead of applying an empirical value for the isentropic efficiency of the expander throughout the two-phase region. This methodology allows for a better assessment of the potential of the PEORC as an alternative to the ORC for industrial waste heat recovery applications. The simulations indicate that the PEORC outperforms the ORC for all the studied operating scenarios. The methodology and results presented in this work may be utilized by the industry as a guide when assessing different technological solutions to increase energy efficiency.

2. Methods

Qualitative Temperature-entropy (T-s) diagrams of the PEORC and the ORC are presented in Fig. 1, where the thermodynamic processes undergone by the Heat Transfer Fluid (HTF) and the Cooling Fluid (CF) are also drawn. As mentioned in the Introduction, the thermodynamic processes of the WF are the same for both power cycles, namely a) 1→2: Adiabatic pumping, b) 2→3: Heat absorption at the evaporator, c) 3→4: Adiabatic expansion, and d) 4→1: Heat rejection at the condenser. The values of the parameters used for the simulations presented herein, along with their descriptions, symbols, and units are listed in Table 1.

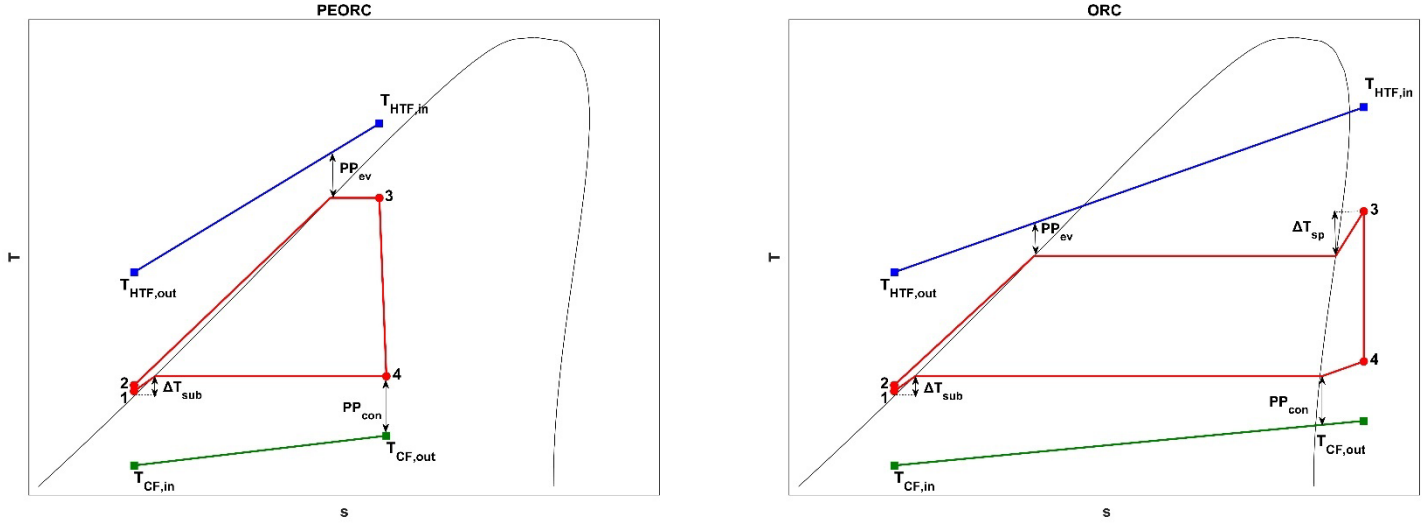

Fig. 1: Qualitative T-s diagrams of the PEORC and the ORC.

In the evaporator, the temperature of the HTF drops from $T_{HTF,in}$ to $T_{HTF,out}$. The temperature of the CF at the inlet of the condenser is equal to $T_{CF,in}$, and it rises to $T_{CF,out}$ at the condenser pinch point, as in Eq. (1). The condensation

temperature T_{con} of the WF is then given by Eq. (2). The calculation of T_{con} leads to the determination of the WF condensation pressure p_{con}.

$$T_{CF,out} = T_{CF,in} + \Delta T_{CF} \quad (1)$$

$$T_{con} = T_{CF,out} + PP_{con} \quad (2)$$

The heat duty $\dot{Q}_{ev}$ at the evaporator is given by Eq. (3), where $c_{p,HTF}$ is the specific heat, under constant pressure, of the of the HTF, and $T_{HTF,out}$ its temperature at the evaporator outlet. Ignoring the heat losses at the evaporator, $\dot{Q}_{ev}$ is also given by Eq. (4), where $\dot{m}_{WF}$ is the mass flowrate of the WF, whereas h_2 and h_3 denote its specific enthalpy at states 2 and 3, respectively.

$$\dot{Q}_{ev} = \dot{m}_{HTF} c_{p,HTF} \left(T_{HTF,in} - T_{HTF,out}\right) \quad (3)$$

$$\dot{Q}_{ev} = \dot{m}_{WF} (h_3 - h_2) \quad (4)$$

Table 1: Parameters for PEORC and ORC simulations.

Parameter	Description [Units]	Value
WF	Working Fluid [-]	R245fa, R1234ze(Z), R1234ze(E)
HTF	Heat Transfer Fluid [-]	H_2O
$\dot{m}_{HTF}$	Mass flowrate of the HTF [kg/s]	2
he_{htf}	HTF pump head [m]	10
PP_{ev}	Pinch point at the evaporator [°C]	5
PP_{con}	Pinch point at the condenser [°C]	5
$T_{HTF,in}$	HTF temperature at the evaporator inlet [°C]	80-100
$T_{CF,in}$	CF temperature at the condenser inlet [°C]	30
$\dot{Q}_{ev}$	Heat duty at the evaporator [kW_{th}]	100-300
CF	Cooling Fluid [-]	Air
ΔT_{CF}	Temperature rise of the CF [°C]	10
ΔT_{sub}	WF sub-cooling at the condenser [°C]	5
ΔT_{sp}	WF superheat at the evaporator in ORC [°C]	1-5
x_3	Quality of the WF at the onset of expansion in PEORC [-]	0.1-0.9
$\eta_{pu,is}$	Pump isentropic efficiency [%]	70
η_{em}	Electromechanical efficiency [%]	90

By applying Eq. (5), the temperature $T_{HTF,pr}$ of the HTF at the end of preheating is calculated, for a given value of the WF evaporation pressure p_{ev}. In Eq. (5), $T_{WF,sat}(p_{ev})$ is the saturation temperature of the WF at p_{ev}. The heat duty $\dot{Q}_{pr}$ of the evaporator is given by Eq. (6), where $h_{l,sat}(p_{ev})$ represents the specific enthalpy of the liquid WF at p_{ev}.

$$PP_{ev} = T_{HTF,pr} - T_{WF,sat}(p_{ev}) \quad (5)$$

$$\dot{Q}_{ev} = \dot{m}_{HTF} c_{p,HTF} \left(T_{HTF,pr} - T_{HTF,out}\right) = \dot{m}_{WF} \left(h_{l,sat}(p_{ev}) - h_2\right) \quad (6)$$

By inspecting Eqs. (3)-(6), two unknown variables are identified, namely $\dot{m}_{WF}$ and p_{ev}. Moreover, a degree of freedom is also pinpointed, i.e. the value of x_3 for the PEORC and of ΔT_{sp} for the ORC. Specifying desired values for x_3 and ΔT_{sp} (within the ranges prescribed in Table 1) allows for the calculation of $\dot{m}_{WF}$ and p_{ev} from the set of Eqs. (3)-(6), for given $\dot{Q}_{ev}$.

The isentropic efficiency $\eta_{ex,is}$ of the expander is given by Eq. (7), where h_4 is the WF's specific enthalpy at state, and $h_{4,is}$ is its specific enthalpy corresponding to its isentropic expansion from state 3 to p_{con}. In ORC simulations a fixed value, equal to 0.70, is used for $\eta_{ex,is}$, and Eq. (7) is used to calculate h_4. On the other hand, in PEORC simulations the semi-empirical thermodynamic model (details about the methodology in Ref. [12]) is run to simulate two-phase expansion as a function of x_3, $\dot{m}_{WF}$, p_{ev}, and p_{con}. In the case of PEORC, h_4 is an output of the two-phase expansion model, and Eq. (7) is applied, as post-processing, to calculate $\eta_{ex,is}$.

$$\eta_{ex,is} = (h_3 - h_4)/(h_3 - h_{4,is}) \quad (7)$$

The shaft power $\dot{w}_{ex}$ generated by the twin-screw expander, and the power $\dot{w}_{pu}$ absorbed by the WF pump are by Eqs. (8) and (9), respectively. The value of h_2 in Eq. (9) is calculated by applying Eq. (10), where $h_{2,is}$ stands for the specific enthalpy of the WF corresponding to its isentropic pumping from state 1 to p_{ev}. On the other hand, h_1 in Eq. calculated as a function of p_{con} and ΔT_{sub}. The power $\dot{w}_{htf}$ absorbed by the HTF pump is calculated by Eq. (11), where is the gravitational acceleration. Finally, the thermal efficiency η_{th} of the power cycle is given by Eq. (12), where $\dot{w}_{net}$ represents the net generated power.

$$\dot{w}_{ex} = \dot{m}_{WF}(h_3 - h_2)\eta_{em} \quad (8)$$

$$\dot{w}_{pu} = \dot{m}_{WF}(h_2 - h_1)/\eta_{em} \quad (9)$$

$$\eta_{pu,is} = (h_{2,is} - h_1)/(h_2 - h_1) \quad (10)$$

$$\dot{w}_{htf} = \dot{m}_{HTF} he_{htf} g/\eta_{em} \quad (11)$$

$$\eta_{th} = \dot{w}_{net}/\dot{Q}_{ev} = (\dot{w}_{ex} - \dot{w}_{pu} - \dot{w}_{htf})/\dot{Q}_{ev} \quad (12)$$

3. Results and Discussion

At first, the variation of $\eta_{ex,is}$ in the PEORC based on the operating conditions is analyzed. This brief analysis is presented because the efficiency of two-phase expansion mainly affects the thermal efficiency of the PEORC, and, consequently, its competitiveness against the standard ORC. The effect of x_3 and $T_{htf,in}$ on $\eta_{ex,is}$ in the PEORC is presented in Fig. 2. As x_3 increases over 0.1 the isentropic efficiency of the expander is improved until the optimal value of $\eta_{ex,is}$ is achieved for a vapor quality between 0.6 and 0.7. This behavior of $\eta_{ex,is}$ indicates that at this x_3 range the WF volume ratio approaches the built-in volume ratio of the modeled expander (details in Ref. [12]). As $T_{htf,in}$ increases, higher $\eta_{ex,is}$ are calculated by the two-phase expansion simulations, indicating that higher operating pressure ratios are favorable. This is because a better match between the pressure at the end of expansion and the pressure at the discharge line can be achieved as the temperature of the heat source increases (under-expasnion losses are minimized). Finally, it must be noted that the effect of the WF type on $\eta_{ex,is}$ is negligible, and, therefore, not presented herein.

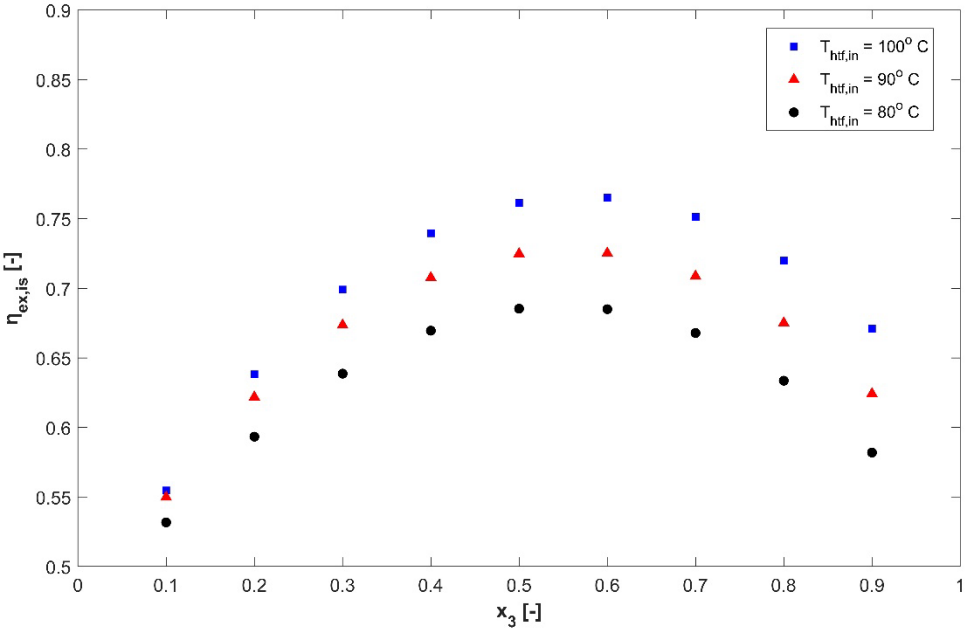

Fig. 2: $\eta_{ex,is}$ as a function of x_3 and $T_{htf,in}$ in PEORC.

In Figs. 3 and 4 η_{th} versus x_3 for different values of $T_{htf,in}$ is presented for $\dot{Q}_{ev}$ equal to 100 and 300 kW_{th}, respectively. As anticipated, based on analysis of the two-phase expansion efficiency, increasing $T_{htf,in}$ leads to improved values of η_{th}. At higher $\dot{Q}_{ev}$ the thermal efficiency decreases. This is caused by the deterioration of the two-phase expander efficiency as $\dot{m}_{WF}$ increases since the leakage flow rates are higher [12], with a negative effect on $\eta_{ex,is}$. For $\dot{Q}_{ev}$ equal to 100 kW_{th} the optimal value of η_{th} is obtained at x_3 approaching 0.6 regardless of $T_{htf,in}$ and the type of the WF. On the other hand, for $\dot{Q}_{ev}$ equal to 300 kW_{th}, there is a variation of the value of x_3 for which the higher η_{th} is calculated. Particularly, as $T_{htf,in}$ drops the optimal x_3 is reduced to values as low as 0.2. Concerning the WF selection, the simulations indicate that R1234ze(Z) and R245fa perform almost identically, and, in any case, more efficiently or equivalently to R1234ze(E).

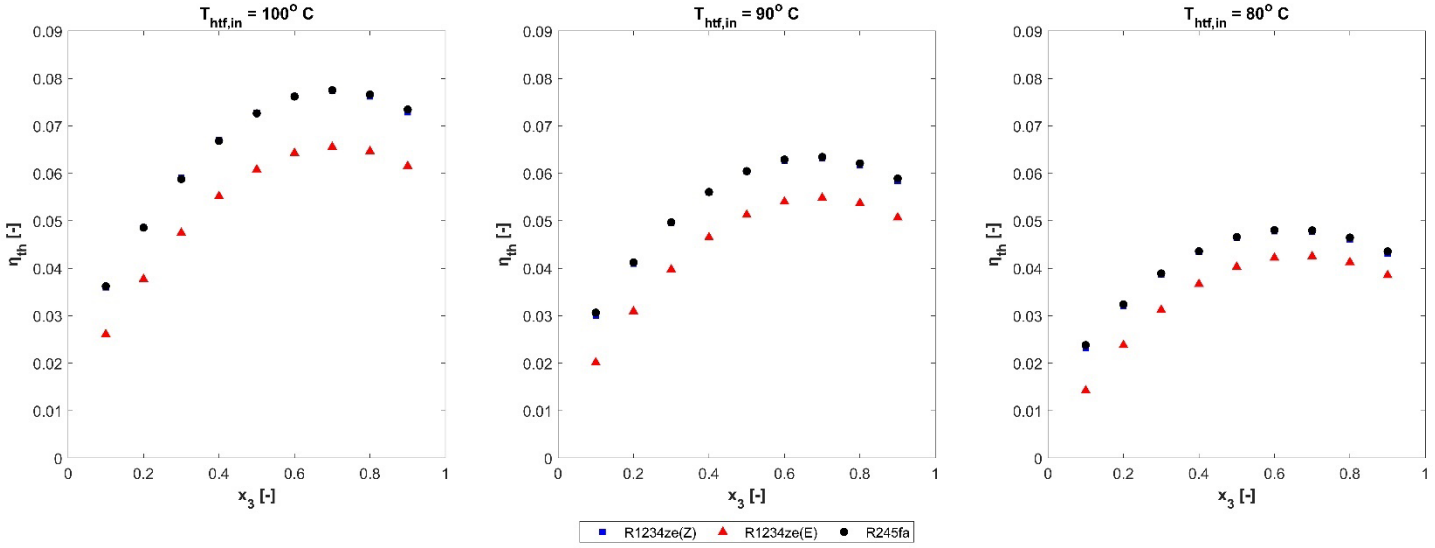

Fig. 3: η_{th} as a function of x_3 in PEORC for different WFs and values of $T_{htf,in}$. $\dot{Q}_{ev} = 100\ kW_{th}$.

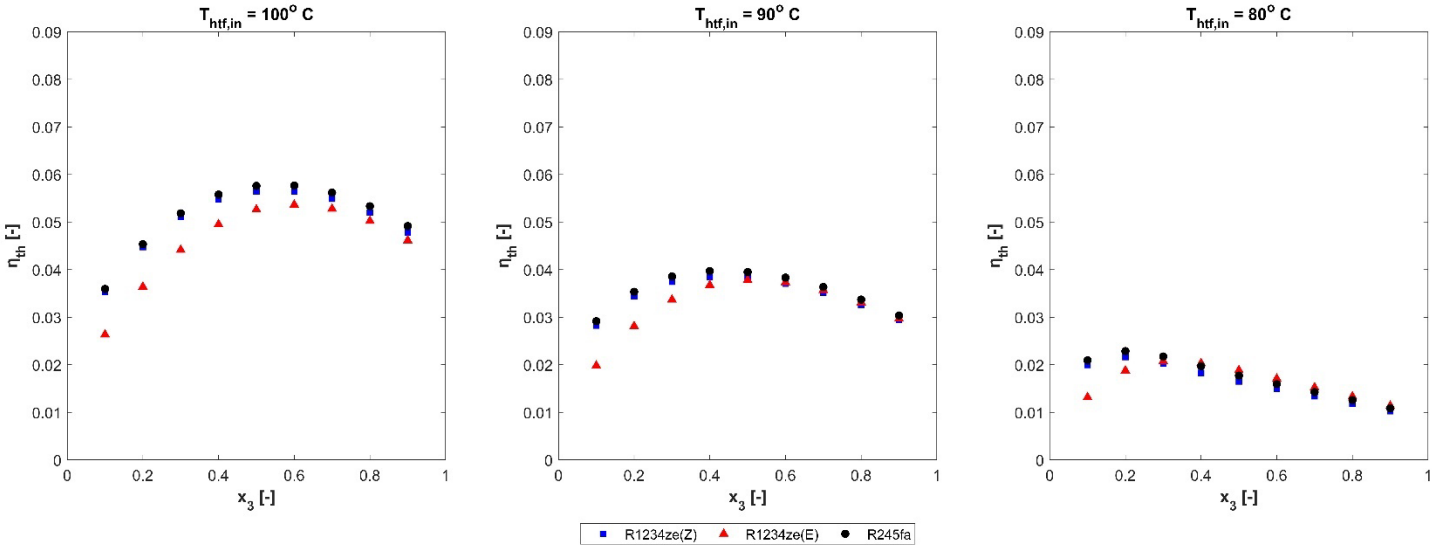

Fig. 4: η_{th} as a function of x_3 in PEORC operation for different WFs and values of $T_{htf,in}$. $\dot{Q}_{ev} = 300\ kW_{th}$.

Overall, it is estimated that the PEORC can achieve a maximum η_{th} equal to 7.75%, 6.34%, and 4.80% for $T_{htf,in}$ equal to 100 ºC, 90 ºC, and 80 ºC, respectively, when $\dot{Q}_{ev}$ equals 100 kW_{th}. The respective values of η_{th} when $\dot{Q}_{ev}$ is equal to 300 kW_{th} are 5.76%, 3.96%, and 2.28%.

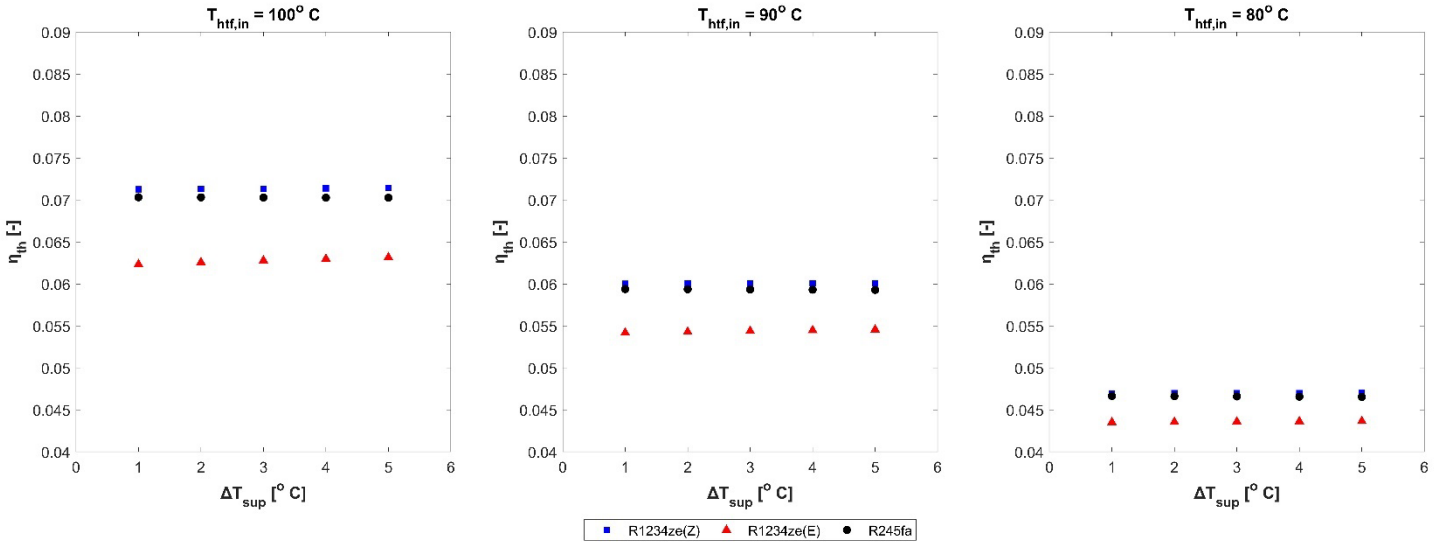

Fig. 5: η_{th} as a function of ΔT_{sp} in ORC operation for different WFs and values of $T_{htf,in}$. $\dot{Q}_{ev} = 100\ kW_{th}$.

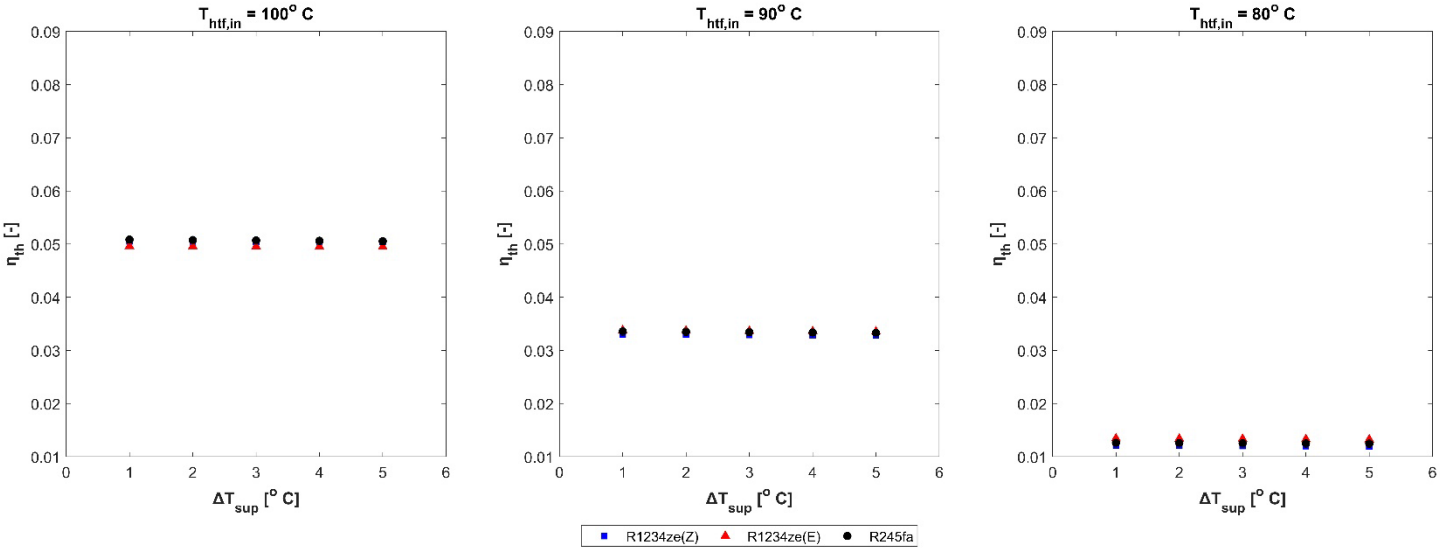

Fig. 6: η_{th} as a function of ΔT_{sp} in ORC operation for different WFs and values of $T_{htf,in}$. $\dot{Q}_{ev} = 300\ kW_{th}$.

The effect of ΔT_{sp} and $T_{htf,in}$ on η_{th} for the ORC operation is presented in Figs. 5 and 6 for $\dot{Q}_{ev}$ equal to 100 kW_{th} and 300 kW_{th}, respectively. The variation of η_{th} as a function of ΔT_{sp} is negligible because the respective difference in the value of p_{ev} is slight. As $T_{htf,in}$ is reduced, η_{th} diminishes because the operating pressure ratio of the power cycle is reduced, with a negative effect on the enthalpy drop of the WF. As $\dot{Q}_{ev}$ increases η_{th} decreases because the value of p_{ev} is reduced for the same value of ΔT_{sp} at the suction port of the expander. As observed in the case of the PEORC,

R1234ze(Z) outperforms or, in the worst case, is as efficient as the other examined WFs for all the examined operating conditions.

Quantitatively, the standard ORC can accomplish a η_{th} equal to 7.13%, 6.00%, and 4.66% when $T_{htf,in}$ equals 100 °C, 90 °C, and 80 °C, respectively, and the heat duty at the evaporator reaches 100 kW_{th}. When $\dot{Q}_{ev}$ is equal to 300 kW_{th} the respective values for the thermal efficiency are 5.06%, 3.34%, and 1.25%.

4. Conclusions

In the present work, a performance comparison of the PEORC and ORC power cycles for low-temperature waste heat recovery was performed, with operating scenarios relevant to the industrial sector. Numerical models of the two power cycle architectures were developed and their thermal efficiency was monitored for different WFs, temperatures of the heat source, and heat duties at the evaporator. Particular attention was on two-phase expansion in the PEORC by applying a dedicated semi-empirical numerical model [12] that highlights the effect of vapor quality, WF mass flow rate, and pressure ratio on the expander's efficiency.

The simulations indicate that the PEORC performs better than the standard ORC under all the examined operating scenarios. The PEORC and ORC can achieve a thermal efficiency in the range of 2.28% to 7.75%, and 1.25% to 7.13%, respectively. This difference in thermal efficiency between the two configurations may be even higher. This is because, for the simulations presented herein, the isentropic efficiency of the expander in the dry vapor region was kept constant and relatively high, and no effects of the operating conditions on the expander performance were considered.

In conclusion, the present work highlighted the potential of the PEORC as a competitive alternative to the standard ORC for low-temperature waste heat recovery. However, additional experimental data in the PEORC are necessary to consolidate its superiority against the ORC, the performance of which is documented in the literature and real-world applications.

Acknowledgment

This research work was supported by the Hellenic Foundation for Research and Innovation (H.F.R.I.) under the "First Call for H.F.R.I. Research Projects to support Faculty members and Researchers and the procurement of high-cost research equipment grant" (Project Number: 1087, Acronym: SOL-art).

References

[1] C. Forman, I.K. Muritala, R. Pardemann, B. Meyer, Estimating the global waste heat potential, Renew. Sustain. Energy Rev. 57 (2016) 1568–1579. https://doi.org/10.1016/j.rser.2015.12.192.

[2] M. Papapetrou, G. Kosmadakis, A. Cipollina, U. La Commare, G. Micale, Industrial waste heat: Estimation of the technically available resource in the EU per industrial sector, temperature level and country, Appl. Therm. Eng. 138 (2018) 207–216. https://doi.org/10.1016/J.APPLTHERMALENG.2018.04.043.

[3] V. Lemort, A. Legros, 12 - Positive displacement expanders for Organic Rankine Cycle systems, in: E. Macchi, M.B.T.-O.R.C. (ORC) P.S. Astolfi (Eds.), Woodhead Publishing, 2017: pp. 361–396. https://doi.org/https://doi.org/10.1016/B978-0-08-100510-1.00012-0.

[4] B.F. Tchanche, G. Lambrinos, A. Frangoudakis, G. Papadakis, Low-grade heat conversion into power using organic Rankine cycles – A review of various applications, Renew. Sustain. Energy Rev. 15 (2011) 3963–3979. https://doi.org/10.1016/J.RSER.2011.07.024.

[5] A. Schuster, S. Karellas, R. Aumann, Efficiency optimization potential in supercritical Organic Rankine Cycles, Energy. 35 (2010) 1033–1039. https://doi.org/10.1016/J.ENERGY.2009.06.019.

[6] R. DiPippo, Ideal thermal efficiency for geothermal binary plants, Geothermics. 36 (2007) 276–285. https://doi.org/10.1016/J.GEOTHERMICS.2007.03.002.

[7] I.K. Smith, Development of the trilateral flash cycle system: Part 1: Fundamental considerations, Proc. Inst. Mech. Eng. Part A J. Power Energy. 207 (1993) 179–194. https://doi.org/10.1243/PIME_PROC_1993_207_032_02.

[8] M.T. White, Cycle and turbine optimisation for an ORC operating with two-phase expansion, Appl. Therm. Eng. 192 (2021) 116852. https://doi.org/https://doi.org/10.1016/j.applthermaleng.2021.116852.

[9] G. Bianchi, S. Kennedy, O. Zaher, S.A. Tassou, J. Miller, H. Jouhara, Numerical modeling of a two-phase twin-screw expander for Trilateral Flash Cycle applications, Int. J. Refrig. 88 (2018) 248–259. https://doi.org/10.1016/J.IJREFRIG.2018.02.001.
[10] H. Öhman, P. Lundqvist, Experimental investigation of a Lysholm Turbine operating with superheated, saturated and 2-phase inlet conditions, in: Appl. Therm. Eng., Pergamon, 2013: pp. 1211–1218. https://doi.org/10.1016/j.applthermaleng.2012.08.035.
[11] I.K. Smith, N. Stošić, C.A. Aldis, Development of the trilateral flash cycle system. Part 3: The design of high-efficiency two-phase screw expanders, Proc. Inst. Mech. Eng. Part A J. Power Energy. 210 (1996) 75–92. https://doi.org/10.1243/pime_proc_1996_210_010_02.
[12] A. Skiadopoulos, G. Kosmadakis, S. Lecompte, M. De Paepe, D. Manolakos, Numerical modeling of flashing in TFC expanders for the efficient exploitation of low-grade heat, Therm. Sci. Eng. Prog. (2023) 102171. https://doi.org/https://doi.org/10.1016/j.tsep.2023.102171.